

Tensor-Based Modulation for Unsourced Massive Random Access

Alexis Decurninge, Ingmar Land and Maxime Guillaud

Abstract—We introduce a modulation for unsourced massive random access whereby the transmitted symbols are rank-1 tensors constructed from Grassmannian sub-constellations. The use of a low-rank tensor structure, together with tensor decomposition in order to separate the users at the receiver, allows a convenient uncoupling between multi-user separation and single-user demapping. The proposed signaling scheme is designed for the block fading channel and multiple-antenna settings, and is shown to perform well in comparison to state-of-the-art unsourced approaches.

I. INTRODUCTION

Massive random access, whereby a large number of transmitters communicate with a single receiver, constitutes a key design challenge for future generations of wireless systems. The considered scenarios typically consider sporadic traffic with small payloads; furthermore, only a fraction of the transmitters are active at a given time. In that context, it is desirable to let users transmit without any prior resource request (grant-free). At the physical layer, this requires a departure from the design assumptions prevailing in current cellular systems [1].

The grant-free random access problem has recently been revisited taking massive connectivity into account (see [2]). One classical approach consists in a functional split at the receiver between activity detection and channel estimation on one hand (typically, based on user-specific pilot sequences) and multi-user equalization and demapping of the information-bearing symbols on the other hand. Another approach lies in ALOHA schemes and their extensions, such as slotted coded ALOHA [3].

Recently, the emergence of unsourced random access [4] has sparked a renewed interest in the problem. In this paradigm, the identity of the active transmitters is not associated with a specific waveform at the physical layer. Theoretical analysis of the unsourced scenario has been done in [4] in the single-in-single-output (SISO) case for an additive white Gaussian noise (AWGN) channel and extended to quasi-static Rayleigh fading in [5]. Several practical schemes have been proposed for this scenario. For the SISO AWGN case, [6] proposed a scheme close to sparse regression codes proposed in [7] where the idea is to see the unsourced access as a very large compressed sensing problem where messages are encoded through sparse vectors. In order to enable reasonable decoding complexity, the

linear compressed sensing mapping is split into blocks while the messages are encoded by a binary outer code. In [8], the authors combined the compressed sensing approach with a multi-user coding scheme, also allowing a low-complexity decoder. Relaxing the AWGN hypothesis and assuming Rayleigh fading, [5] proposes a scheme based on a low-density parity check (LDPC) code using a belief propagation decoder. The MIMO case with Rayleigh fading is addressed in [9] as well as in [10] wherein encoders inspired from compressed sensing were used while adapting the decoder to the MIMO setup.

In this article, we propose a modulation suitable for massive multiple access, where multi-user multiplexing is handled through the use of tensor algebra. Specifically, each user transmits a sequence that is associated to a rank-one tensor. The receiver observes the linear combination of these signals weighted by the respective channel realizations, which itself can be interpreted as a tensor summing a number of rank-one components equal to the number of active users. This structure allows the receiver to separate the users using a classical tensor decomposition, without requiring a separate activity detection or channel estimation step; the channels are estimated jointly with the data by the receiver. The benefits of the proposed approach are:

- user separation can be performed by the receiver without relying on pilot sequences, thus circumventing the difficult problem of pilot sequence design for grant-free access, and without involving any knowledge about the discrete nature of the modulation;
- the proposed scheme applies to a broad class of multiple-access channels (including AWGN and block-fading) and generalizes to multiple-antenna receivers while benefiting from spatial diversity, without relying on any assumption on the fading distribution.

II. UNSOURCED MASSIVE RANDOM ACCESS BACKGROUND AND CHANNEL MODEL

We consider the transmission from K single-antenna transmitters to a single receiver equipped with N antennas. Let us consider a block of T channel uses, during which we assume that only $K_a \ll K$ users are active (where K_a is still typically large) and simultaneously transmit a payload of B information bits each. The set of active users is a random subset of the K users (hence its cardinality K_a is a random variable) and, following the unsourced random access paradigm [4], we will work under the assumption that all users use the same constellation $\mathcal{C} = \{\mathbf{c}_1, \dots, \mathbf{c}_{2^B}\}$ containing 2^B elements. Under this assumption, the receiver

The authors are with the Mathematical and Algorithmic Sciences Laboratory, Paris Research Center, Huawei Technologies France. e-mail: *firstname.lastname@huawei.com*.

can only decode the messages up to a permutation over the user indices¹.

Let $\mathbf{h}_k \in \mathbb{C}^N$ denote the channel from user k . We assume in this paper a block-fading model whereby the channel realizations remain constant over the considered block of T channel uses, and is a priori unknown to both the transmitters and the receiver. Let us further assume without loss of generality (w.l.o.g.) that the active users are indexed by $1, \dots, K_a$. We let $\mathbf{s}_k \in \mathcal{C} \subset \mathbb{C}^T$ denote the sequence of complex baseband symbols transmitted by user k over T channel uses, and $\mathbf{W} \in \mathbb{C}^{T \times N}$ the noise realization. The users are assumed block-synchronous, therefore the signal $\mathbf{Y} \in \mathbb{C}^{T \times N}$ received by the N antennas over the T channel accesses can be written as $\mathbf{Y} = \sum_{k=1}^{K_a} \mathbf{s}_k \mathbf{h}_k^T + \mathbf{W}$. Let $\mathbf{y}, \mathbf{w} \in \mathbb{C}^{TN}$ denote the respective vectorized versions of \mathbf{Y} and \mathbf{W} . We can rewrite the received signal using the Kronecker product operator (denoted by \otimes) as

$$\mathbf{y} = \sum_{k=1}^{K_a} \mathbf{s}_k \otimes \mathbf{h}_k + \mathbf{w}. \quad (1)$$

III. TENSOR-BASED MODULATION (TBM)

A. Tensor Structure

In this work, we propose to design the constellation \mathcal{C} according to a tensor construction. Here, we merely consider tensors to be multi-dimensional data structures, which can be seen as the generalization of matrices to dimensions greater than 2 (see [11] for an introduction). Specifically, let us consider a complex-valued tensor of order d (which can be construed as d -dimensional array of complex scalars) of dimensions T_1, \dots, T_d . Note that the $\prod_{i=1}^d T_i$ scalars forming the tensor can also be stored sequentially in a vector (see [12, Sec. 2.4]). The corresponding vectorization operator defines an isomorphism between the space of (T_1, \dots, T_d) -dimensional tensors and the space of $(\prod_{i=1}^d T_i)$ -dimensional vectors, endowed with the respective sum operations. For notational convenience, throughout the paper we will use the vectorized representation while referring to algebraic arguments applying in the space of tensors.

In the proposed approach, we assume that the block-length T can be factored as $T = \prod_{i=1}^d T_i$ for some $d \geq 2$ and $T_1, \dots, T_d \geq 2$, and constrain \mathbf{s}_k to be the vectorized representation of a rank-1 tensor of dimensions T_1, \dots, T_d , characterized by the existence of vectors $\mathbf{x}_{i,k} \in \mathbb{C}^{T_i}$ for $1 \leq i \leq d$, such that

$$\mathbf{s}_k = \mathbf{x}_{1,k} \otimes \dots \otimes \mathbf{x}_{d,k} \in \mathbb{C}^{\prod_{i=1}^d T_i} = \mathbb{C}^T. \quad (2)$$

We further constrain each $\mathbf{x}_{i,k}$ to be an element of a sub-constellation \mathcal{C}_i defined as a discrete subset of \mathbb{C}^{T_i} , i.e. $\mathbf{x}_{i,k} \in \mathcal{C}_i \subset \mathbb{C}^{T_i}$. The resulting vector constellation \mathcal{C} is a discrete subset of \mathbb{C}^T comprised of all possible combinations

¹Note that the identity of the transmitting user can be included in the message (e.g. in the form of $\lceil \log_2 K \rceil$ bits). In that case, the total number of users K has an impact on the achieved spectral efficiency since the data payload is reduced to $B - \lceil \log_2 K \rceil$ per user. Here, we ignore that aspect and focus on the unsourced problem.

of elements of the sub-constellations, i.e.

$$\mathcal{C} = \left\{ \mathbf{x}_1 \otimes \dots \otimes \mathbf{x}_d : \mathbf{x}_1 \in \mathcal{C}_1, \dots, \mathbf{x}_d \in \mathcal{C}_d \right\}. \quad (3)$$

Substituting (2) in (1), the received signal becomes

$$\mathbf{y} = \underbrace{\sum_{k=1}^{K_a} \mathbf{x}_{1,k} \otimes \dots \otimes \mathbf{x}_{d,k}}_{\triangleq \mathbf{y}_0} \otimes \mathbf{h}_k + \mathbf{w} \in \mathbb{C}^{TN}, \quad (4)$$

where we let \mathbf{y}_0 denote the noise-free received signal.

A tensor is said to be rank- r whenever r is the smallest integer such that the tensor can be written as a sum of r rank-1 tensors [12, Sec. 3.1]. Considering eqs. (2) and (4), note that each user transmits a rank-1 tensor of order d , while \mathbf{y}_0 is the vector representation of a tensor of order $d+1$ and dimensions T_1, \dots, T_d, N having rank at most K_a .

B. Tensor Decomposition, Identifiability and User Separation

The proposed modulation design is motivated by the fact that the decomposition of a tensor into a sum of rank-1 components (known as the canonical polyadic decomposition, or CPD) is unique up to a permutation over the components under mild conditions. Furthermore, tensors of order 3 or more can attain high rank even for moderate tensor sizes (conditions linking the maximum rank to the tensor size differ significantly from the matrix case, and will be detailed below). This hints at the possibility for the TBM to achieve a high degree of multiplexing, while using the CPD to separate the signal components related to each user.

Let us consider in more detail the maximum rank and unique decomposability conditions of the noise-free tensor in eq. (4). We have the following definition:

Definition 1 (CPD uniqueness and rank): The (T_1, \dots, T_d, N) -dimensional tensor represented by \mathbf{y}_0 admits a unique rank- K_a CPD if for any set $\{\mathbf{x}'_{1,k} \in \mathbb{C}^{T_1}, \dots, \mathbf{x}'_{d,k} \in \mathbb{C}^{T_d}, \mathbf{h}'_k \in \mathbb{C}^N, 1 \leq k \leq K'_a\}$ with $K'_a \leq K_a$ such that

$$\sum_{k=1}^{K'_a} \mathbf{x}'_{1,k} \otimes \dots \otimes \mathbf{x}'_{d,k} \otimes \mathbf{h}'_k = \mathbf{y}_0, \quad (5)$$

then it holds that $K'_a = K_a$ and there exists a permutation σ such that $\mathbf{x}'_{1,k} \otimes \dots \otimes \mathbf{x}'_{d,k} \otimes \mathbf{h}'_k = \mathbf{x}_{1,\sigma(k)} \otimes \dots \otimes \mathbf{x}_{d,\sigma(k)} \otimes \mathbf{h}_{\sigma(k)}$.

According to [13], there exists an upper bound \bar{R} to the rank of uniquely decomposable tensors, in the sense that the set of rank- K_a tensors for which the CPD is not unique has measure zero if $K_a < \bar{R}$. Let us restate the main result of [13] using our notations. For tensors of size T_1, \dots, T_d, N , let us assume w.l.o.g. that $T_1 \geq T_2 \geq \dots \geq T_d$ and define

$$R^0 = \left\lceil \frac{TN}{N + \sum_{i=1}^d (T_i - 1)} \right\rceil \quad (6)$$

(which is known as the *expected generic rank*), as well as

$$R^1 = 2 - N + N \prod_{i=2}^d T_i - \sum_{i=2}^d (T_i - 1), \quad \text{and} \quad (7)$$

$$R^2 = 1 + T - \sum_{i=1}^d (T_i - 1). \quad (8)$$

According to [13, Th. 1.1], we have²

$$\bar{R} = \begin{cases} R^1 - 1 & \text{for } T_1 \geq R^1 \\ R^2 - 1 & \text{for } N \geq R^2 \\ R^0 & \text{otherwise,} \end{cases} \quad (9)$$

$$(10)$$

$$(11)$$

where eqs. (9) and (10) correspond to the unbalanced tensor size case of [13, Th. 1.1]. Note that for both unbalanced cases, it holds that $\bar{R} \leq R^0$, i.e. the balanced case favors higher rank with respect to the unbalanced case. The practical consequence of the above result is that in the noise-free case, performing a CPD allows the receiver to separate users with high probability whenever $K_a < \bar{R}$.

Note that Definition 1 considers tensor decomposition in a continuous domain (i.e. $\mathbf{x}_{i,k} \in \mathbb{C}^{T_i}$). A definition more directly related to the communication problem at hand, in the sense that it takes into account the discrete nature of the \mathcal{C}_i , is as follows:

Definition 2 (Discrete identifiability): The noise-free received tensor is *identifiable in the discrete case* if for any set $\{\mathbf{x}'_{1,k} \otimes \dots \otimes \mathbf{x}'_{d,k} \in \mathcal{C}, \mathbf{h}'_k \in \mathbb{C}^N, 1 \leq k \leq K'_a\}$ with $K'_a \leq K_a$ and

$$\sum_{k=1}^{K'_a} \mathbf{x}'_{1,k} \otimes \dots \otimes \mathbf{x}'_{d,k} \otimes \mathbf{h}'_k = \mathbf{y}_0 \quad (12)$$

then it holds that $K'_a = K_a$ and there exists a permutation σ such that $\mathbf{x}'_{i,k} = \mathbf{x}_{i,\sigma(k)}$ and $\mathbf{h}'_k = \mathbf{h}_{\sigma(k)}$.

Clearly, Definition 2 is appropriate for the communications problem at hand³, while the CPD uniqueness condition is unnecessarily strong (there might be tensors which are discretely identifiable but do not admit a unique CPD). Definition 1 is nonetheless relevant, since i) it constitutes a sufficient condition for the discrete identifiability, and ii) it is simpler than Definition 2 since it is independent from the design of the discrete constellation \mathcal{C} .

C. Design of the sub-constellations

We now discuss the design of the information-bearing sub-constellations $\mathcal{C}_1, \dots, \mathcal{C}_d$. Observe that the rank-1 tensor $\mathbf{x}_{1,k} \otimes \dots \otimes \mathbf{x}_{d,k} \otimes \mathbf{h}_k$ is equal to $\alpha_1 \mathbf{x}_{1,k} \otimes \dots \otimes \alpha_d \mathbf{x}_{d,k} \otimes \alpha_{d+1} \mathbf{h}_k$ with $\alpha_1, \dots, \alpha_{d+1} \in \mathbb{C}$ whenever $\prod_{i=1}^{d+1} \alpha_i = 1$. This indicates that, even if the CPD perfectly recovers the rank-1 component associated to each transmitter, the information-bearing components $\mathbf{x}_{1,k}, \dots, \mathbf{x}_{d,k}$ can only be retrieved up to a set of d complex scalar multiplicative coefficients, effectively providing d parallel (non-interfering) non-coherent SISO block-fading channels to each active user. In order to account for this scalar indeterminacy, each sub-constellation \mathcal{C}_i can either i) embed at least one reference symbols, or ii) rely on a Grassmannian codebook design suitable for the single-user non-coherent block-fading case [14], [15].

²Note that the proof mechanism used in [13] limits the result to tensors of size $N \prod_i T_i \leq 15000$, however there is no indication that it does not hold more generally. Note also that we have omitted a few exceptions applying to some specific tensor sizes from our restatement of [13, Th. 1.1].

³We remark that because of the unsourced nature of the scheme, the case of several users transmitting the same payload leads to a failure in the discrete identifiability of \mathbf{y}_0 . However, as noted in [4], this occurs with low probability when the payload size B is large, and can be completely avoided if the payload includes a unique user identifier.

IV. MULTI-USER RECEIVER

A. Maximum Likelihood (ML) Decoder

Let us consider the joint multi-user ML detection problem under the assumption that the noise \mathbf{w} is Gaussian with i.i.d. coefficients. For the sake of clarity, we will first assume that the number of active users K_a is known to the receiver. The channel realizations \mathbf{h}_k can be considered as nuisance parameters here, and the ML estimator writes

$$\{\hat{\mathbf{x}}_{i,k}\} = \operatorname{argmin}_{\{\mathbf{x}_{i,k} \in \mathcal{C}_i\}} \min_{\{\mathbf{h}_k \in \mathbb{C}^N\}} \left\| \mathbf{y} - \sum_{k=1}^{K_a} \mathbf{x}_{1,k} \otimes \dots \otimes \mathbf{x}_{d,k} \otimes \mathbf{h}_k \right\|_2^2. \quad (13)$$

The optimization over $\{\mathbf{h}_k\}$ is a least squares problem, and therefore has a closed form solution. Solving the discrete problem in (13) via an exhaustive search, however, requires 2^{BK_a} evaluations of the objective function, which makes it a task of formidable complexity.

B. Two-Step Decoder

To circumvent the complexity issue, we propose to exploit the tensor structure of the proposed modulation, which allows a simpler two-step decoding process, as follows.

Multi-user separation: First, an approximate CPD with K_a components is performed, in order to recover an approximate version (denoted by $\hat{\mathbf{z}}_{i,k}$) of the $\mathbf{x}_{i,k}$; specifically, (13) is relaxed to yield the rank- K_a tensor approximation problem

$$\{\hat{\mathbf{z}}_{i,k}, \hat{\mathbf{h}}_k\} = \operatorname{argmin}_{\substack{\mathbf{z}_{i,k} \in \mathbb{C}^{T_i}, 1 \leq i \leq d \\ \mathbf{h}_k \in \mathbb{C}^N}} \left\| \mathbf{y} - \sum_{k=1}^{K_a} \mathbf{z}_{1,k} \otimes \dots \otimes \mathbf{z}_{d,k} \otimes \mathbf{h}_k \right\|_2^2. \quad (14)$$

Single-user demapping: The second step consists in performing single-user demapping independently for each user, i.e. for each $1 \leq k \leq K_a$ solve the discrete problem

$$\operatorname{argmin}_{\substack{\mathbf{x}_{i,k} \in \mathcal{C}_i, 1 \leq i \leq d \\ \mathbf{h}_k \in \mathbb{C}^N}} \left\| \hat{\mathbf{z}}_{1,k} \otimes \dots \otimes \hat{\mathbf{z}}_{d,k} \otimes \hat{\mathbf{h}}_k - \mathbf{x}_{1,k} \otimes \dots \otimes \mathbf{x}_{d,k} \otimes \mathbf{h}_k \right\|_2^2. \quad (15)$$

Solving (15) over \mathbf{h}_k (see details in Appendix A) indicates that the problem is separable into d instances of the minimum chordal distance demapping problem typical of non-coherent modulations:

$$\hat{\mathbf{x}}_{i,k} = \operatorname{argmax}_{\mathbf{x}_{i,k} \in \mathcal{C}_i} \frac{|\mathbf{x}_{i,k}^H \hat{\mathbf{z}}_{i,k}|}{\|\hat{\mathbf{z}}_{i,k}\| \|\mathbf{x}_{i,k}\|}. \quad (16)$$

Solving (16) can still be complex if an exhaustive search over the elements of \mathcal{C}_i is performed. However, this complexity can be significantly decreased through the use of structured constellations such as the one from [15].

C. Random User Activation

In the random access scenario, the number of active users K_a is random and unknown to the base station. This can be addressed by performing the approximate CPD (14) using an upper bound \bar{K}_a to K_a (assuming that the user activation

probability is known, \overline{K}_a can be chosen such that $\overline{K}_a \geq K_a$ is fulfilled with arbitrarily high probability). The subsequent demapping of the \overline{K}_a rank-1 tensors resulting from the approximate CPD will yield \overline{K}_a messages, among which at most K_a correspond to actually transmitted messages. One option is then to discard the messages based on power thresholding on $|\mathbf{s}_k|$; note however that, even if the noise level can be assumed low, this option is not well mathematically justified, because of the lack of a tensor equivalent to the Eckart–Young theorem [16]. Another option is to use a binary code to add redundancy at the transmitter, and to check whether the decoded binary sequences actually fulfill the code constraints. In this case, the choice of the code should emphasize the error detection capability, since it will be used by the receiver to discard messages that do not correspond to an active user, i.e. for which the demapper output is close to uniform i.i.d. bits.

V. ACHIEVABLE DEGREES OF FREEDOM

In order to establish the number of degrees of freedom (DoF) achievable by the proposed TBM, let us consider the case of asymptotically high signal-to-noise ratio (SNR), i.e. we assume that the noise-free signal \mathbf{y}_0 is available at the receiver. The DoF achievability proof relies on a random coding argument, in the sense that we assume that the elements of the sub-constellations \mathcal{C}_i are independently drawn from an absolutely continuous distribution. We will also assume that the channel realizations \mathbf{h}_k are drawn from an absolutely continuous distribution. These two assumptions ensure that the received tensor is generic, for which case the CPD is almost surely unique whenever $K_a < \overline{R}$, according to the results cited in Section III-B.

A. Per-User DoF

As already pointed out, the uniqueness of the CPD is defined in terms of the rank-1 components, however each factor $\mathbf{x}_{j,k}$ can only be recovered up to a complex scalar coefficient. Nonetheless, the uniqueness result can be extended to the sub-constellations by considering that the $\mathbf{x}_{j,k}$ are representatives of Grassmannian variables. More specifically, for all $1 \leq i \leq d$, let $G(T_i, 1)$ denote the Grassmannian of lines in dimension T_i , i.e. the set of 1-dimensional linear subspaces of \mathbb{C}^{T_i} , and let us consider \mathbf{x}_i as a representative of the corresponding point in $G(T_i, 1)$ (see [14] for background information on Grassmannian codebooks). Note that every rank-1 component $\mathbf{x}_{1,k} \otimes \dots \otimes \mathbf{x}_{d,k} \otimes \mathbf{h}_k$ maps to a unique point of $G(T_1, 1) \times \dots \times G(T_d, 1) \times G(N, 1)$. Consequently, whenever $K_a < \overline{R}$, the proposed scheme allows the noise-free communication of d complex Grassmannian variables in $G(T_1, 1) \dots G(T_d, 1)$ respectively, for each active user (the component in $G(N, 1)$ corresponds to the channel, and does not carry information). As shown in [14], a variable in $G(T, 1)$ has $T-1$ DoF. Summing across the sub-constellations indicates that the TBM approach allows the noise-free communication of $\sum_{i=1}^d (T_i - 1)$ DoF per active user.

B. Sum-DoF

The total DoF achieved in the system is obtained by summing up the per-user DoF; therefore, it is a function of K_a . Since every active user contributes $\sum_{i=1}^d (T_i - 1)$ DoF up to the maximum number of users for which the rank- K_a tensor is almost surely identifiable, the sum-DoF is

$$D_{\text{TBM}}(K_a) = K_a \sum_{i=1}^d (T_i - 1) \quad \text{for } K_a \leq \overline{R} - 1. \quad (17)$$

Clearly, the highest sum-DoF is attained for $K_a = \overline{R} - 1$, and is $D_{\text{TBM}}(\overline{R} - 1) = (\overline{R} - 1) \sum_{i=1}^d (T_i - 1)$. Moreover, using the fact that $K_a \leq \overline{R} - 1 \leq R^0 - 1 < \frac{TN}{N + \sum_{i=1}^d (T_i - 1)}$, we can upper bound the DoF independently from the tensor size by

$$D_{\text{TBM}}(K_a) < N(T - K_a). \quad (18)$$

Another upper bound to the sum-DoF can be obtained by allowing the K_a transmitters to cooperate; in that case, the considered set-up is equivalent to a non-coherent point-to-point MIMO channel with K_a transmit antennas and N receive antennas, which has an achievable DoF of [14]

$$D_{\text{coop}}(K_a) = M^*(T - M^*) \quad (19)$$

where $M^* = \min(K_a, N, \lfloor T/2 \rfloor)$. If we assume that $N < \min(K_a, T/2)$, the cooperative bound from eq. (19) yields $D_{\text{coop}}(K_a) = N(T - N)$; comparing with eq. (18) therefore highlights a loss of at least $N(K_a - N)$ DoF due to the uncoordinated access.

Figure 1 depicts the sum-DoF per channel use achievable using different tensor sizes; specifically, for fixed values of T and N , it depicts the points $(K_a, \frac{D_{\text{TBM}}(K_a)}{T})$ for values of K_a ranging from 1 to $\overline{R} - 1$, achievable using various choices of the factorization $T = \prod_{i=1}^d T_i$. The bound (18) and the cooperative upper bound are also depicted. Note that this figure highlights an interesting trade-off between spectral efficiency and the maximum degree of contention: in the regime of large K_a (i.e. when (18) is tight), using a tensor size supporting a higher number of users results in a decrease in both sum-DoF and per-user DoF. TBM configurations achieving the highest per-user DoF (on the left of the figure) correspond to unbalanced tensors (eqs. (9)-(10)); in this case, the upper bound $K_a < \overline{R}$ is more restrictive than (18).

VI. SIMULATION RESULTS

The performance of the proposed TBM has been evaluated through simulations. Our simulation includes a Bose–Chaudhuri–Hocquenghem (BCH) binary code applied to the messages transmitted by each user. In addition to its error correction capability, the binary code allows for more refined multi-user decoding strategies (such as the turbo-like approach used below). In order to facilitate the comparison with results available in the literature, we assume here that the number of active users is known to the receiver through a genie, and therefore set $\overline{K}_a = K_a$ in our simulations. Note however that error detection can be instrumental in the case where K_a is unknown a priori.

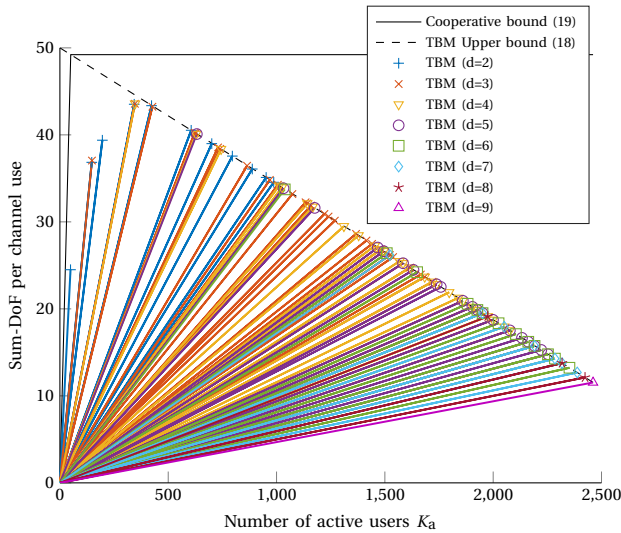


Fig. 1. Achievable sum-DoF per channel use ($D_{\text{TBM}}(K_a)/T$) vs. K_a for different tensor sizes (d and T_i), for $T = 3200$ and $N = 50$. The markers denote the case $K_a = \bar{R} - 1$, while the slope of the lines going through the origin represents the per-user DoF.

A. Modulation Parameters

Our set-up assumes a payload of $B = 96$ information bits at each transmitter (referred to as a message), which are BCH-encoded into a codeword of length $B_{\text{tot}} = 110$ bits; the BCH code can correct up to 2 bit errors thanks to the $B_{\text{BCH}} = 14$ bits of redundancy. Bit-to-symbol mapping is performed as depicted on Fig. 2, i.e. the B_{tot} coded bits are split into d sets of respectively B_1, \dots, B_d bits, corresponding to the d tensor dimensions. The i -th set, comprised of B_i bits, is mapped to an element of the sub-constellation \mathcal{C}_i ; we used the Grassmannian constellation design from [15] for the \mathcal{C}_i , due to the availability of a low-complexity approximate demapper. Finally, the vector symbol \mathbf{s}_k is formed by computing the Kronecker product (2).

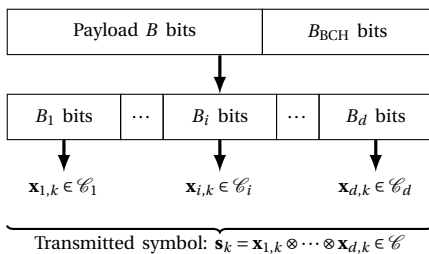


Fig. 2. Bit mapping for user k

We consider two tensor sizes for the TBM, namely $(T_1, T_2) = (64, 50)$ and $(T_1, T_2, T_3, T_4, T_5) = (8, 5, 5, 4, 4)$. According to [15, Lemma 1], the minimum distance between the elements of \mathcal{C}_i is maximized when the B_i are proportional to $T_i - 1$. In order to approximately fulfill this requirement, the $B_{\text{tot}} = B + B_{\text{BCH}} = 110$ bits are split according to $(B_1, B_2) = (62, 48)$ and $(B_1, B_2, B_3, B_4, B_5) = (37, 21, 21, 16, 15)$ respectively

for the two considered cases. In both cases, the dimension of \mathbf{s}_k is $T = \prod_{i=1}^d T_i = 3200$ channel uses.

B. Receiver Details

Taking into account the non-convexity of the objective function of (14), the receiver used in the simulations consists of two iterations of the two-step decoder described in Section IV-B. At the first iteration, user separation (14) and demapping (16) are performed in order to recover the coded binary stream; then, for each binary vector fulfilling exactly the BCH constraints, the corresponding message is deemed valid. Thus, at the first iteration, the BCH code is used for error detection only. At iteration 2, user separation (14) is performed a second time, during which the symbols corresponding to the messages decoded at iteration 1 are excluded from the optimization variables and replaced by their hard decision values. After user separation and demapping, the binary vectors are BCH decoded: if decoding is successful (now using the error correction capability of the BCH code), the corresponding message is deemed valid; if decoding fails, the vector is discarded. Let $\hat{\mathcal{L}}$ denote the list of messages deemed valid at either of the two iterations, while \mathcal{L} denotes the list of messages actually transmitted by the active users. Since the messages can be decoded only up to a permutation over the users, the considered error metric is the average message error ratio (MER),

$$\text{MER} = \mathbb{E} \left[\min \left(\underbrace{\frac{|\mathcal{L} \setminus \hat{\mathcal{L}}|}{|\mathcal{L}|}}_{\text{average ratio of missed messages}}, \underbrace{\frac{|\hat{\mathcal{L}} \setminus \mathcal{L}|}{|\hat{\mathcal{L}}|}}_{\text{average ratio of phantom messages}}, 1 \right) \right]. \quad (20)$$

The MER accounts for two types of error events: (i) a transmitted message was not detected; (ii) a detected message was not transmitted. The two error events may be correlated, therefore we limit the MER value to at most 1.

In our implementation, the approximate CPD (14) is implemented using the nonlinear least square algorithm combined with a preconditioner proposed in [17].

C. Performance Results – Unsourced Scenario

The results in this section have been obtained for complex Gaussian i.i.d. (across the users and the receive antennas) fading channels with unit variance. The entries of the noise \mathbf{w} are i.i.d complex Gaussian with variance σ^2 , while the transmitted symbols are normalized according to the considered energy per bit to noise ratio $E_b/N_0 = \frac{\|\mathbf{s}_k\|^2}{B\sigma^2}$ for all k .

In Figure 3, the performance of TBM is compared to the compressed sensing-based approach proposed in [9], for K_a ranging from 50 to 650, and $E_b/N_0 = 0$ dB. It can be observed that tensor-based methods maintain a low MER for K_a ranging up to 650, while the design from [9] exhibits a large MER already for $K_a \approx 100$. In order to illustrate the role of the binary code, we also consider an *uncoded* set-up, not involving any binary code ($B_{\text{BCH}} = 0$). In this case, a single decoding stage (eqs. (14)-(16)) is performed

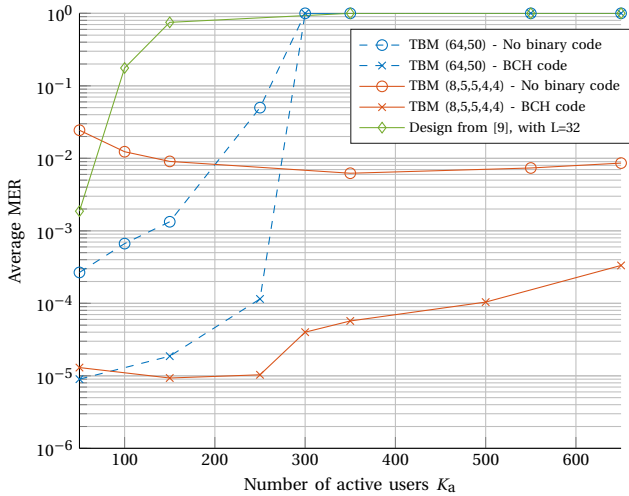


Fig. 3. Average per-user MER vs. number of active users for a BS with $N = 50$ antennas and $E_b/N_0 = 0$ dB.

at the receiver, and $\hat{\mathcal{L}}$ always consists of K_a messages). Also observe that TBM with sizes $(8,5,5,4,4)$ yields consistently superior performance to what is achieved using tensors of sizes $(64,50)$, which seems to indicate that, for a fixed T , designs with higher d are preferable.

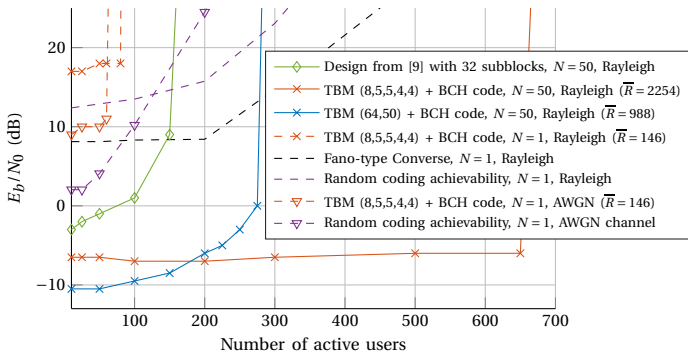


Fig. 4. Minimum E_b/N_0 required to achieve $\text{PUPE} \leq 0.1$ vs. number of active users for $T = 3200$.

Figure 4 depicts the E_b/N_0 required to achieve a target error rate, for $N = 50$ and $N = 1$ antennas. To facilitate comparison with the existing results, we now focus on the average per user probability of error (PUPE) [4], defined as

$$\text{PUPE} = \mathbb{E} \left[\frac{|\mathcal{L} \setminus \hat{\mathcal{L}}|}{|\mathcal{L}|} \right], \quad (21)$$

and depict the E_b/N_0 required to achieve a PUPE lower or equal to 0.1. For TBM, the value of \bar{R} is included in the legend. We compare to the approach from [9] with 32 subblocks. We also include the single-antenna receiver case for comparison, for which theoretical bounds are available, such as a Fano-type converse bound and a random coding achievability bound, both from [18, Appendix B] in the Rayleigh fading case, and the achievability bound of [4] for

the AWGN case. We observe that TBM benefits from spatial diversity (the number of users that can be successfully decoded increases with N , as suggested by the DoF analysis), and allows to achieve very high multiplexing gains for the case of multiple receive antennas, with reasonable packet loss rate and E_b/N_0 . For instance, for $N = 50$, it allows up to 650 active users over a Rayleigh fading channel, which translates into a spectral efficiency of 19.5 bits/channel access.

D. Performance Results – Sourced Scenario

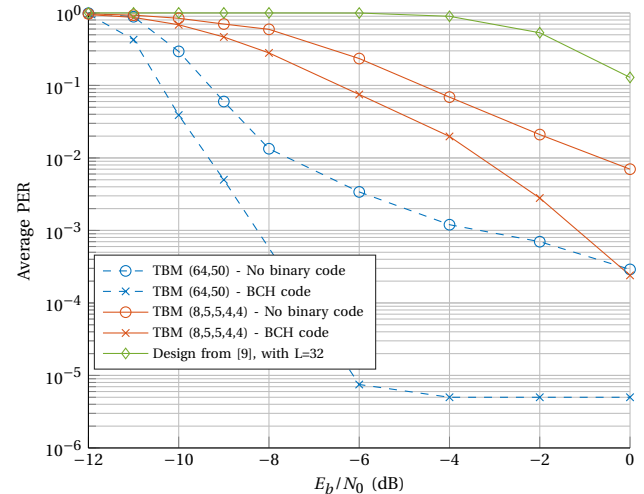


Fig. 5. PER vs. E_b/N_0 for $T = 3200$, $N = 50$, $K_a = 100$ and $K = 8192$.

Let us now consider the case where every transmitter embeds its identity (ID) in the payload, in addition to the $B = 96$ information bits. We assume that $K_a = 100$ users are active, out of a total of $K = 8192$ users; therefore, $B_{\text{ID}} = \log_2(K) = 13$ bits are required to encode the user ID. Hence, each user transmits a total of $B_{\text{tot}} = B_{\text{ID}} + B = 109$ bits when no binary code is used and $B_{\text{tot}} = B_{\text{ID}} + B + B_{\text{BCH}} = 123$ bits when the BCH code mentioned in Section VI-A is used. At the receiver side, in addition to the unsourced decoding procedure described in Section VI-B, the transmitting users are identified based on the ID embedded in the decoded payload. This allows to evaluate the packet error rate (PER) metric as in a sourced scenario. If several messages with the same user ID are decoded, they are discarded and counted as an error. The resulting PER (averaged over the active users) is depicted in Figure 5; the error floor at high E_b/N_0 is due to the lack of optimality of the solution to the non-convex problem (14). It is noticeable that, when using BCH code and in the case of $K_a = 100$ active users, TBM $(8,5,5,4,4)$ PER is higher than TBM $(64,50)$ in the sourced scenario while they have similar MER in the unsourced scenario, hence the former is more impacted by the addition of the B_{ID} identity bits. This may be explained by the number of DoF which is higher in the latter making its use more suitable for denser constellations.

REFERENCES

- [1] Y. Wu, X. Gao, S. Zhou, W. Yang, Y. Polyanskiy, and G. Caire. (2019) Massive access for future wireless communication systems. [Online]. Available: <https://arxiv.org/abs/1910.12678>
- [2] L. Liu, E. G. Larsson, W. Yu, P. Popovski, C. Stefanovic, and E. de Carvalho, "Sparse signal processing for grant-free massive connectivity," *IEEE Signal Processing Magazine*, vol. 35, no. 5, pp. 88–99, 2018.
- [3] E. Paolini, C. Stefanovic, G. Liva, and P. Popovski, "Coded random access: How coding theory helps to build random-access protocols," *IEEE Communications Magazine*, vol. 53, no. 6, pp. 144–150, 2015.
- [4] Y. Polyanskiy, "A perspective on massive random-access," in *IEEE Int. Symp. Inf. Theory (ISIT)*, 2017.
- [5] S. S. Kowshik, K. Andreev, A. Frolov, and Y. Polyanskiy, "Energy efficient random access for the quasi-static fading MAC," in *IEEE Int. Symp. Inf. Theory (ISIT)*, 2019.
- [6] A. Fengler, P. Jung, and G. Caire. (2019) SPARCs for unsourced random access. [Online]. Available: <https://arxiv.org/abs/1901.06234>
- [7] A. Barron and A. Joseph, "Sparse superposition codes are fast and reliable at rates approaching capacity with gaussian noise," *Symp. Q. J. Mod. Foreign Lit.*, pp. 1–70, 2011.
- [8] A. Pradhan, V. Amalladinne, A. Vem, K. R. Narayanan, and J.-F. Chamberland. (2019) A joint graph based coding scheme for the unsourced random access Gaussian channel. [Online]. Available: <https://arxiv.org/abs/1906.05410v1>
- [9] A. Fengler, G. Caire, P. Jung, and S. Haghghatshoar. (2019) Massive MIMO unsourced random access. [Online]. Available: <https://arxiv.org/abs/1901.00828>
- [10] V. Shyianov, F. Bellili, A. Mezghani, and E. Hossain. (2020) Massive unsourced random access based on uncoupled compressive sensing: Another blessing of massive MIMO. [Online]. Available: <https://arxiv.org/abs/2002.03044>
- [11] P. Comon, "Tensors: a brief introduction," *IEEE Signal Processing Magazine*, vol. 31, no. 3, pp. 44–53, 2014.
- [12] T. Kolda and B. Bader, *Tensor decompositions and applications*. SIAM Review, 2009.
- [13] L. Chiantini, G. Ottaviani, and N. Vannieuwenhoven, "An algorithm for generic and low-rank specific identifiability of complex tensors," *SIAM Journal on Matrix Analysis and Applications*, vol. 35, no. 4, p. 1265–1287, 2014.
- [14] L. Zheng and D. N. C. Tse, "Communication on the Grassmann manifold: A geometric approach to the noncoherent multiple-antenna channel," vol. 48, no. 2, pp. 359–383, Feb. 2002.
- [15] K.-H. Ngo, A. Decurninge, M. Guillaud, and S. Yang, "Cube-split: A structured Grassmannian constellation for non-coherent SIMO communications," *IEEE Transactions on Wireless Communications*, vol. 19, no. 20, Mar. 2020.
- [16] J. Draisma, G. Ottaviani, and A. Tocino, "Best rank-k approximations for tensors: generalizing Eckart–Young," *Research in the Mathematical Sciences*, vol. 5, no. 27, 2018.
- [17] L. Sorber, M. V. Barel, and L. De Lathauwer, "Optimization-based algorithms for tensor decompositions: Canonical polyadic decomposition, decomposition in rank-(Lr;Lr;1) terms, and a new generalization," *SIAM J. Optim.*, vol. 23, no. 2, pp. 695–720, 2013.
- [18] S. Kowshik, K. Andreev, A. Frolov, and Y. Polyanskiy. (2019) Energy efficient coded random access for the wireless uplink. [Online]. Available: <https://arxiv.org/abs/1907.09448>

APPENDIX A

DETAILS ON THE SINGLE-USER DECODER

Fixing $\mathbf{x}_{i,k} \in \mathcal{C}_i$ for all i, k , and solving (15) with respect to \mathbf{h}_k , yields

$$\mathbf{h}_k^* = \frac{(\mathbf{x}_{1,k} \otimes \cdots \otimes \mathbf{x}_{d,k})^H (\hat{\mathbf{z}}_{1,k} \otimes \cdots \otimes \hat{\mathbf{z}}_{d,k})}{\|\mathbf{x}_{1,k} \otimes \cdots \otimes \mathbf{x}_{d,k}\|^2} \hat{\mathbf{h}}_k. \quad (22)$$

Substituting (22) into the objective function of (15), and applying the property that $\mathbf{a} \otimes \mathbf{b} = \text{vec}(\mathbf{a}\mathbf{b}^T)$ for arbitrary vectors \mathbf{a} and \mathbf{b} to both terms, we get

$$\begin{aligned} & \|\hat{\mathbf{z}}_{1,k} \otimes \cdots \otimes \hat{\mathbf{z}}_{d,k} \otimes \hat{\mathbf{h}}_k - \mathbf{x}_{1,k} \otimes \cdots \otimes \mathbf{x}_{d,k} \otimes \mathbf{h}_k^*\| \\ &= \|\text{vec}((\hat{\mathbf{z}}_{1,k} \otimes \cdots \otimes \hat{\mathbf{z}}_{d,k}) \hat{\mathbf{h}}_k^T) - \text{vec}((\mathbf{x}_{1,k} \otimes \cdots \otimes \mathbf{x}_{d,k})(\mathbf{h}_k^*)^T)\| \\ &= \|P_{\mathbf{x}}(\hat{\mathbf{z}}_{1,k} \otimes \cdots \otimes \hat{\mathbf{z}}_{d,k}) \hat{\mathbf{h}}_k^T\|_2^2, \end{aligned} \quad (23)$$

where we define the projection matrix $P_{\mathbf{x}} = \mathbf{I}_T - \frac{(\mathbf{x}_{1,k} \otimes \cdots \otimes \mathbf{x}_{d,k})(\mathbf{x}_{1,k} \otimes \cdots \otimes \mathbf{x}_{d,k})^H}{\|\mathbf{x}_{1,k} \otimes \cdots \otimes \mathbf{x}_{d,k}\|^2}$. Using $\|\mathbf{a}\mathbf{b}^T\|_2^2 = \|\mathbf{a}\|_2^2 \|\mathbf{b}\|_2^2$ and the fact that $P_{\mathbf{x}}$ is a projector, the optimization problem (15) is equivalent to

$$\max_{\mathbf{x}_{i,k} \in \mathcal{C}_i, \forall i} \frac{\|(\mathbf{x}_{1,k} \otimes \cdots \otimes \mathbf{x}_{d,k})(\mathbf{x}_{1,k} \otimes \cdots \otimes \mathbf{x}_{d,k})^H (\hat{\mathbf{z}}_{1,k} \otimes \cdots \otimes \hat{\mathbf{z}}_{d,k})\|_2^2}{\|\mathbf{x}_{1,k} \otimes \cdots \otimes \mathbf{x}_{d,k}\|^4}. \quad (24)$$

Finally, using $(\mathbf{a} \otimes \mathbf{b})^H (\mathbf{a}' \otimes \mathbf{b}') = (\mathbf{a}^H \mathbf{a}') (\mathbf{b}^H \mathbf{b}')$ we obtain

$$\max_{\mathbf{x}_{i,k} \in \mathcal{C}_i, \forall i} \prod_{i=1}^d \frac{|\mathbf{x}_{i,k}^H \hat{\mathbf{z}}_{i,k}|}{\|\hat{\mathbf{z}}_{i,k}\| \|\mathbf{x}_{i,k}\|} \quad (25)$$

which is clearly separable, and yields (16).